


Impact of penetrating collisions of plasma ions on spectral line shapes

Thomas A. Gomez 

*Department of Astrophysical and Planetary Sciences, University of Colorado Boulder, Boulder, Colorado 80305, USA;
National Solar Observatory, University of Colorado Boulder, Boulder, Colorado 80303, USA;
and Department of Astronomy, University of Texas at Austin, Austin, Texas 78712, USA*

Evgeny Stambulchik 

Faculty of Physics, Weizmann Institute of Science, Rehovot 7610001, Israel

Jackson White 

*Department of Astronomy, University of Texas at Austin, Austin, Texas 78712, USA
and Computational Physics Division, Los Alamos National Laboratory, Los Alamos, New Mexico 87545, USA*



(Received 27 October 2023; accepted 16 April 2024; published 2 May 2024)

Spectral-line-broadening models have been moving towards including full Coulomb interactions between the atom and plasma, replacing the commonly used dipole approximation. The effects of the full Coulomb interaction have been thoroughly explored for plasma electrons, resulting in redshifts of spectral lines in high-energy-density plasmas. We explore the impact of a full Coulomb treatment on ion broadening. Penetrating collisions due to ions do not significantly impact the linewidths. The most significant aspect is the appearance of quasimolecular resonances in the far line wings, such as those previously observed in white-dwarf spectra. We identify several problems with the existing models. The most direct implementation causes the quasimolecular features to appear at the wrong photon energies. It is possible to include the detailed molecular structure, but this currently requires the Anderson-Talman approximation, which ignores the N -body properties of the plasma. We find that N -body effects can substantially broaden these quasimolecular features and even shift them, depending on the plasma conditions. We conclude that penetration of ions into the spatial extent of the radiator wave function does not strongly affect the usual diagnostics and may have a moderate to weak effect on opacity. The Rosseland mean opacity is weighted towards low-opacity regions of a spectrum, where these quasimolecular features are found.

DOI: [10.1103/PhysRevA.109.052804](https://doi.org/10.1103/PhysRevA.109.052804)

I. INTRODUCTION

Understanding atomic behavior in hot dense matter (HDM) is essential for understanding astrophysical [1,2] and laboratory plasmas [3,4], but calculations of perturbed atomic structure in the complex environments of HDM plasmas are challenging. Such calculations, however, are necessary because the broadening of spectral lines is important for determining opacity since broader spectral lines result in larger Rosseland means. Gomez *et al.* [5] showed that additional broadening of the Ly $_{\alpha}$ line resulted in a redistribution of flux in the white-dwarf-atmosphere model [2]. This redistribution may be responsible for the current discrepancies between determining surface parameters using different methods [6,7]. Furthermore, spectral-line-shape models are an important diagnostic tool for determining plasma parameters, in particular, density.

Spectral-line-broadening models often employ the dipole approximation [8] that replaces the full Coulomb interaction

$$V_{\text{atom-plasma}} = \sum_p \frac{q_a q_p}{|\vec{r}_a - \vec{r}_p|} \quad (1)$$

with the inner product of the atomic dipole moment \vec{d}_a and the electric field of the plasma \vec{E}_{plasma} ,

$$V_{\text{atom-plasma}} \approx -\vec{d}_a \cdot \vec{E}_{\text{plasma}}. \quad (2)$$

The a and p subscripts stand for the bound electron and a plasma particle (ion or electron), respectively. The dipole approximation has been nearly ubiquitous since the 1960s due to its convenience in separating the atomic and plasma degrees of freedom. In fact, this approximation gives rise to the name Stark broadening [9].

There are many useful quantities for characterizing the plasma. One is the Wigner-Seitz radius

$$r_{\text{WS},s} = \left(\frac{3}{4\pi n_s} \right)^{1/3} \quad (3)$$

for plasma species s (electrons or ions), where n_s is the density of that species. Some other important quantities that help determine the properties of the plasma include the coupling

$$\Gamma_s = \frac{q_s^2}{r_{\text{WS},s} k_B T}, \quad (4)$$

the Debye screening length

$$\lambda_D = \sqrt{k_B T / 4\pi n_e q_e^2}, \quad (5)$$

and the ratio of the electron Wigner-Seitz radius [Eq. (3)] to the Debye length [10] $a = r_{\text{WS},e} / \lambda_D$. The parameter a is a proxy for the number of particles inside the Debye screening

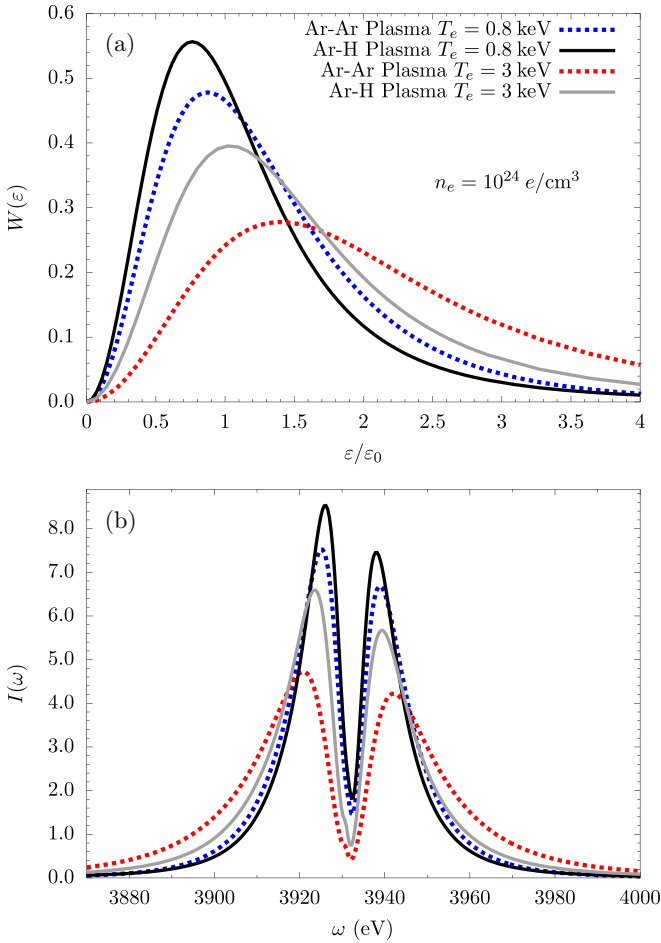


FIG. 1. Demonstration of the weak dependence of spectral line shape (Ar XVIII Ly _{β}) on plasma composition under the dipole approximation. (a) Comparison of the microfield distributions of pure argon plasma and an argon impurity in a hydrogen plasma. (b) The resulting spectral line shapes are slightly modified, but not on the level that would be easily discernible by experiments.

length, where $a = 0$ is an ideal plasma and $a \gg 1$ is a strongly coupled plasma that usually indicates the failure of the Debye approximation. A useful quantity for the dipole approximation in spectral line broadening (in addition to the screening) is the characteristic microfield strength

$$\epsilon_0 = \frac{q_e}{r_{WS,e}^2}, \quad (6)$$

defined specifically in terms of the electron charge and electron Wigner-Seitz radius.

Spectral line shapes depend on the plasma composition. This is demonstrated in Fig. 1, where two different compositions are compared. In Fig. 1(a) microfield calculations from the adjustable-parameter exponential approximation [11] at typical inertial-confinement-fusion plasma conditions are shown, demonstrating that in a pure Ar plasma, there is a slight tendency for higher values of the microfield to be sampled more. Figure 1(b) demonstrates the resulting changes in the spectral line profiles, showing that the spectral linewidths [e.g., the full width at half maximum (FWHM)] in the static-ion approximation (calculated from the BALROG code [5])

are only weakly dependent on the plasma composition. Note that the differences in the microfield distributions and profiles become larger at higher temperatures, where both Γ_i and a have decreased, as exemplified by the $T_e = 3$ keV conditions in Fig. 1.

It has also been established that line profiles are affected by the composition through ion dynamics. This was experimentally demonstrated in the work of Wiese *et al.* [12], where lighter mass plasma particles contributed to a larger ion dynamics effect, causing additional broadening. The effect of ion dynamics is substantial, leading to major increases in the full width at half maximum for α lines [13]. Major efforts went into capturing this effect in neutral hydrogen line shapes using simulation techniques [14,15]. Ion dynamics is also seen in hot dense plasmas where spectral lines of highly ionized mid-Z elements experience substantial broadening from fully ionized lighter elements [16].

The composition of plasma can have yet another impact on spectral line shapes. When the distance between plasma ions becomes comparable to the spatial extent of the bound electron's wave function, quasimolecular resonances are formed. These resonances are readily observed in UV spectra of white dwarfs [17,18] and λ Boötis stars [19], as well as in the laboratory [20]. The strengths, shapes, and positions of these resonances depend on the velocities and charges of the ions in the plasma.

There has already been some effort to model the quasimolecular resonances through detailed two-center models [21]. A critique that can be made about these models is that they solve for ion broadening only and convolve their profiles with an electron-broadening profile. Furthermore, these models only account for two-body interactions.

Another way to study the penetrative effects of plasma particles that more easily includes the N -body dynamics of the plasma is by using the full Coulomb interaction in line-shape calculations. Much of this work has focused on full Coulomb treatments of electron broadening. It has led to a number of successes, including linewidth reduction [22] that brings consistency between various approaches [23]. Another significant result is the plasma polarization shift [24], a redshift arising from the nuclear charge screening. The latter effect provides an important diagnostic tool for solid-density plasmas [25] and resolves [26] the previously identified problem with Stark shifts of the Paschen α line of He⁺ [4].

While it is known that quasimolecular resonances appear in the wings of these spectral lines, more can be explored, especially regarding the composition of the plasma. Including fully penetrating collisions means that exotic quasimolecular pairings are formed in plasmas. For example, in the plasmas produced by the Fe-opacity experiments [27], Fe₂³⁴⁺, Mg₂²²⁺, and Fe-Mg²⁸⁺ quasimolecules would exist. These would differ from the type of quasimolecules seen in the real solar interior, where the most common type of quasimolecule would involve Fe-H pairings.

In this paper we explore the effects the full Coulomb interaction between the radiating atom and the plasma ions have on spectral lines. It is important to emphasize that these calculations include electron and ion broadening together and self-consistently. We look at this effect using two methods: computer simulations and semianalytic calculations. We find

that the inclusion of the full Coulomb method does not substantially change the line shape in the core except at extremely high densities. These calculations produce quasimolecular resonances in the wings of the line shapes, but at inaccurate energies. The remainder of the paper is organized as follows. Section II describes line-shape calculations that account for the full Coulomb interactions. Section III highlights some results of these line-shape calculations performed for neutral hydrogen and hydrogenlike oxygen and argon in fusion plasmas. Section IV discusses the results. A summary and our conclusions are given in Sec. V.

II. FULL COULOMB INTERACTION

Historically, line-shape theory has often simplified the Coulomb interaction between the atom and the charged plasma particles with the dipole approximation. The dipole approximation has several advantages, the principal being that it factorizes the interaction so that the atomic and plasma parts of the interaction can be computed separately. The dipole approximation, however, assumes that the atom is infinitely small, meaning that if plasma particles come too close to the radiating atom, the interaction becomes divergent. This leads, in particular, to an overestimate of the electron broadening [22] in ionized radiators and becomes a motivation for strong-collision cutoff criteria. We note that the contribution of the nondipole terms in the full Coulomb interaction partly compensates for the reduction of the dipole broadening [22]. Furthermore, because the dipole approximation neglects the penetration effects of the plasma particles, it does not predict the shift of the spectral lines due to the zero average charge of the plasma inside the radiator [24]. The importance of the shifting of ionic spectral lines due to penetrating electrons has been demonstrated [25,26].

Using the full Coulomb interaction for perturbing plasma ions modifies line shapes differently than electrons do. Because of their smaller mass, electrons move through the plasma much faster than ions. As a result, electrons are often treated within the impact approximation and ions are often treated in the static limit [28]. However, this statement is not universally applicable. It is well known that electrons are in the static limit in the wings of spectral lines [29]. Quasistatic behavior from electrons can also be seen in the core of lines. For example, in some of the cases previously explored in [30], electrons exhibited quasistatic behavior for H_β at $T_e = 1$ eV and $n_e = 10^{19}$ cm $^{-3}$. Standard-theory line shapes that include ion dynamics are usually corrections on the static-limit [31,32]. This means that at far distances, the ions still (statically) interact with the radiator via the dipole interaction. Only quasistatic interactions at close range significantly split the energy from its zero value in a way that does not result in a Lorentzian line shape.

The full Coulomb interaction between two particles is defined by [cf. Eq. (1)]

$$\frac{q_1 q_2}{|\vec{r}_1 - \vec{r}_2|} = q_1 q_2 \sum_{k=0}^{\infty} \frac{r_{<}^k}{r_{>}^{k+1}} P_k(\cos \gamma), \quad (7)$$

where $r_{<} = \min(r_1, r_2)$, $r_{>} = \max(r_1, r_2)$, γ is the angle between \vec{r}_1 and \vec{r}_2 , and $P_k(x)$ is the k th-order Legendre

polynomial containing all of the angular information. In line broadening, however, it is imperative that the effect of plasma correlations be included [8], either by explicitly accounting for those correlations or by the Debye-screening approximation [33]. The screened Coulomb interaction is evaluated using the partial-wave expansion [34,35]

$$\begin{aligned} & \frac{q_1 q_2}{|\vec{r}_1 - \vec{r}_2|} e^{-|\vec{r}_1 - \vec{r}_2|/\lambda_{\text{scr}}} \\ &= -\frac{q_1 q_2}{\lambda_{\text{scr}}} \sum_{k=0}^{\infty} (2k+1) j_k\left(\frac{ir_{<}}{\lambda_{\text{scr}}}\right) h_k^{(1)}\left(\frac{ir_{>}}{\lambda_{\text{scr}}}\right) P_k(\cos \gamma), \end{aligned} \quad (8)$$

where $j_k(x)$ and $h_k^{(1)}(x)$ are the spherical Bessel functions and spherical Hankel functions of the first kind, respectively. In the limit $\lambda_{\text{scr}} \rightarrow \infty$, Eq. (8) becomes Eq. (7). It is typical that the screening length is taken to be the Debye length [Eq. (5)]. We note that the full Coulomb treatment results in finite potentials, and no minimum radius cutoffs to avoid a divergent potential are necessary.

In this study, two different codes, SIMU and BALROG, are used. SIMU is a simulation method and BALROG is a semianalytic method. We describe each of them below.

In the simulation method, SIMU, the full Coulomb interaction is accounted for using the method of Stambulchik and Iglesias [35]. Simulation methods like SIMU use a classical simulation to generate electric-field histories, which are then used to solve the Schrödinger equation [14,15]. This procedure is repeated averaged over many simulations. When, during the simulation, a plasma particle enters a small sphere with a radius R_{FC} , the atomic-plasma perturbation is evaluated exactly according to Eq. (8). The R_{FC} needs to be at least a few times the typical extent [36]

$$\bar{r} = [3n^2 - l(l+1)]/2Z \quad (9)$$

of the wave functions of the states included in the calculations. Once outside R_{FC} , the simulation method resorts to the usual multipole expansion [37,38]. One particular advantage of the simulation method is its ability to handle the presence of multiple particles simultaneously inside R_{FC} .

We also present calculations using a semianalytic method BALROG [5]. BALROG, like many semianalytic methods, separates the electron and ion contributions to the broadening (e.g., Ref. [39]), where the latter is treated within the static-ion approximation. The electron broadening uses the relaxation theory of Fano [40] and treats the plasma electrons quantum mechanically. BALROG already uses the full Coulomb interaction like Refs. [22,24], where the ion interactions remained in the dipole approximation. BALROG is distinct from past quantum relaxation-theory calculations because it includes (radiationless) dielectronic recombination [41] and solves the required T matrices exactly instead of applying the usual second-order Taylor expansion. This is notable because the T -matrix solutions contained H^- resonances in neutral hydrogen, resulting in additional broadening of the far wings of the Ly_α lines. The contribution of the ions to the broadening is accounted for by integration over electric microfields [39],

$$I(\omega) = \int_0^\infty d\vec{\varepsilon} W(\vec{\varepsilon}) J(\vec{\varepsilon}, \omega), \quad (10)$$

where $I(\omega)$ is the intensity of the spectra, $\bar{\varepsilon}$ is the ion microfield, $W(\bar{\varepsilon})$ is the probability of that microfield occurring, and $J(\bar{\varepsilon}, \omega)$ is the spectrum at that given microfield, containing all of the electron broadening. Thus, the ions are treated in the quasistatic approximation in this model.

In this work, BALROG is updated to take into account the full Coulomb interaction with ions. This is done by assuming that treating only the nearest ion by the full Coulomb interaction suffices. This is facilitated by the assumption that the high-electric-field limit of $W(\bar{\varepsilon})$ is dominated by the nearest neighbor above some threshold electric field. This threshold electric field ε_{FC} is defined as

$$\varepsilon_{FC} = q_i/R_{FC}^2, \quad (11)$$

where q_i is the charge of the ion species and, similar to the simulations, R_{FC} is defined to be some threshold where the effects of the full Coulomb interaction become important. The primary difference between this semianalytic method and the simulation method is that in the former, at most one ion is assumed to be inside R_{FC} and the ions are static. The simulation method allows for both dynamic ions and for there to be more than one ion inside of R_{FC} . The technique that BALROG uses is not dissimilar from the work of Leboucher-Dalimier *et al.* [42], where both methods use the quasistatic and nearest-neighbor approximations. Where the work of Leboucher-Dalimier *et al.* [42] differs from this work is that they solve the multicenter problem exactly, whereas BALROG (as well as SIMU) uses an atomic basis.

This single-perturber approximation is certainly valid at low densities but fails at higher densities. The reason for this is that the probability of finding two perturbing particles inside the small radiator wave function becomes vanishingly small compared to the likelihood of finding a single perturber. However, as the density increases, this probability rises. This single-perturber approximation is valid when the Wigner-Seitz radius r_{WS} is much larger than a typical extent of the wave function,

$$\bar{r} \ll r_{WS}. \quad (12)$$

As an example, Fig. 2 shows the statistics regarding this assumption on oxygen at $n_e = 10^{23} \text{ e/cm}^3$ where oxygen is an impurity in a proton plasma. For this case, $\bar{r} = 1.69a_0$ for $n = 3$, while r_{WS} is $2.5a_0$, which is less than twice \bar{r} . Here we show a histogram of the number of protons inside the critical radius R_{FC} . While having no protons inside, R_{FC} has a probability over 50% for weak fields $|\bar{\varepsilon}| < \varepsilon_{FC}$, there is still a significant chance (greater than 40%) that there will be at least one electron inside the wave function of the radiating atom. This is because there is some cancellation due to a proton just outside R_{FC} but on the opposite side of the radiator to produce a low field. Furthermore, the most probable scenario is that the strong field is generated by a single proton inside R_{FC} . However, the probability that two protons are inside R_{FC} is still around 30%.

III. RESULTS

We show some results on how the ion penetrating collisions affect the line shapes of selected elements.

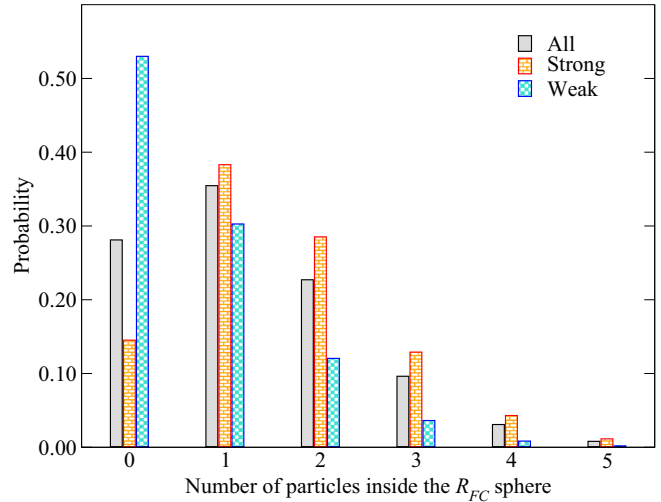


FIG. 2. Statistics for the number of protons inside $R_{FC} = 3 \text{ a.u.}$ for O VIII at $T_e = 180 \text{ eV}$ and $n_e = 10^{23} \text{ e/cm}^3$. The yellow bars, labeled “Strong,” indicate the distribution of protons for electric microfields that are greater than ε_{FC} [defined in Eq. (11)] and the blue bars, labeled “Weak,” are the number of protons inside R_{FC} for fields less than ε_{FC} .

A. Neutral hydrogen

In recent advances in spectral-line-broadening models, one thing has been wonderfully consistent: the shape of the H_β line. Figure 3 demonstrates the remarkable insensitivity to penetrating collisions, further confirming some results from Gomez *et al.* [5], who showed a similar result when applying a full Coulomb treatment to electron broadening. Here we demonstrate that not only the FWHM remains unchanged, but even the detailed line shape does. Therefore, we conclude that H_β can continue to be used as an accurate diagnostic even if the model uses the dipole approximation.

However, this is not to say that the penetration of ions into the hydrogen atom wave function has no effect. The presence of quasimolecular resonances in the wings of hydrogen line

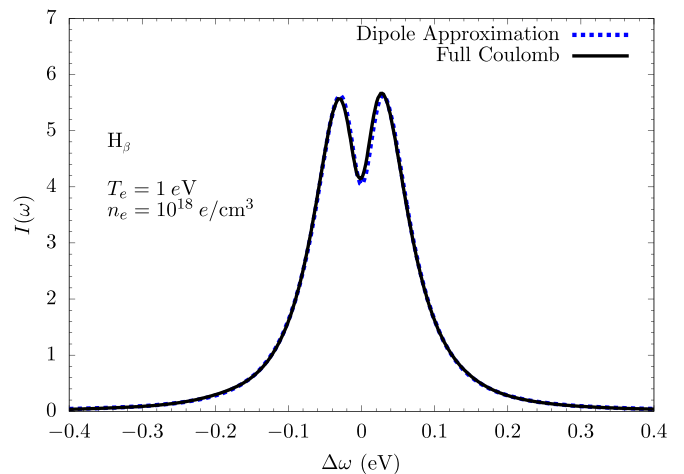


FIG. 3. SIMU calculation of the neutral hydrogen H_β line under two different treatments of plasma interactions. The shape of the H_β line of neutral hydrogen is unaffected by penetrating ions.

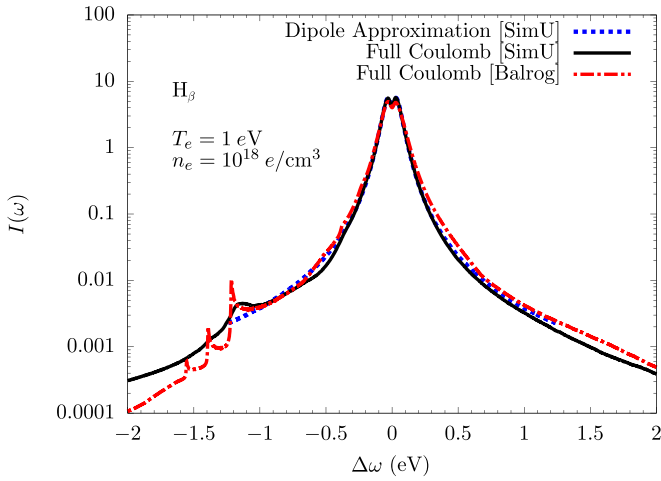


FIG. 4. Demonstration of quasimolecular features in the wings of H_β with simulation (SIMU) and semianalytic (BALROG) codes. BALROG does not include ion dynamics, so the features are far sharper, making them easy to distinguish and identify.

shapes is well documented. Indeed, full Coulomb calculations of the ion-atom interaction result in these quasimolecular resonances. These are demonstrated in Fig. 4, where we show both the simulation (SIMU) and semianalytic calculations (BALROG). SIMU naturally includes ion dynamics and shows these resonances as broad features. To confirm that these are indeed the quasimolecular features, we also show a BALROG calculation that does not include any ion dynamics and indeed the features line up very well. For the conditions demonstrated in Fig. 4, the calculations of BALROG are reasonably accurate because the criterion in Eq. (12) is satisfied for $n = 4$: $r_{WS} = 117a_0$, while $\bar{r} = 24a_0$. Quasimolecular features are expected to be observed in plasmas where the optical depth is high and cores of the spectral lines are strongly saturated.

B. H-like oxygen at solar interior conditions

The opacity of solar material at solar-interior conditions is of significant interest. Much of the research in this area is focused on the mysterious enhancements of opacity from Fe-peak elements [27,43]. We turn our attention to oxygen, the dominant opacity at the base of the solar convection zone [44].

In Fig. 5 we show BALROG calculations [5] of the oxygen Ly_β and Ly_γ lines with penetrating collisions for different mixtures: O, He, and H. It is apparent that the spectral lines undergo significant changes. The BALROG calculations, because there is no ion dynamics at present, show a significant resonance in the Ly_β profile at approximately 760 eV for H perturbors. SIMU does not show this same strong feature at 760 eV, nor is the FWHM reduced by the same amount that BALROG predicts. SIMU shows an extremely broad resonance at about 755 eV, meaning that ion dynamics dominates this feature. The resonances in the SIMU calculations are most easily seen in Fig. 6 in log-log scale. The wing behavior of line profiles calculated under the dipole approximation in log-log scale is shown by straight lines. Any deviation from this straight-line behavior indicates the presence of a resonance. Therefore, once the N -body dynamics of the problem is included, the penetration of ions into the radiator wave function

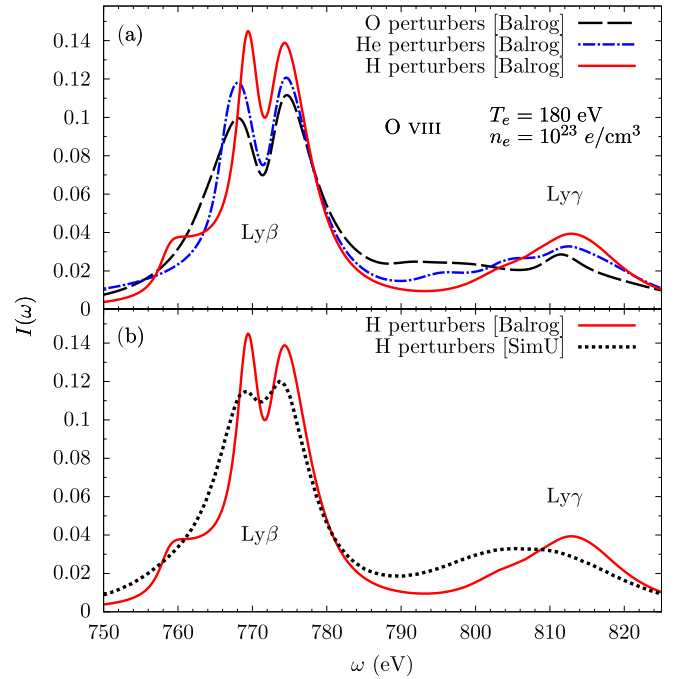


FIG. 5. (a) Oxygen Ly_β and Ly_γ spectral line shapes with three different plasma compositions: pure oxygen (black dashed line), O impurity in He plasma (blue dot-dashed line), and O impurity in H plasma (red solid line). The BALROG calculation shows a distinctive resonance at approximately 760 eV that only appears in the H plasma. Pure O and He plasmas do exhibit resonances such as those in Fig. 4, but they are farther down the line wing. (b) Comparison of methods between BALROG and SIMU. SIMU does not show the same narrowing of the Ly_β or Ly_γ lines as BALROG does and the molecular resonance is weaker. This is likely due to N -body effects being important (see Fig. 2).

results in hardly perceptible changes in the Ly_β profile and would result in a slight enhancement of the red side of the profile.

We also note that the differences in predicted line shape between BALROG and SIMU are more pronounced for Ly_γ . Not only is the line much broader, but it also appears to be shifted by a significant amount. This shift cannot be explained by simply the plasma polarization shift due to the electrons, which is the same in both models. Close examination of the BALROG calculation in Fig. 5(b) shows a quasimolecular resonance at 803 eV, which coincides with the point that SIMU predicts that the intensity starts to decrease for Ly_γ . From this we conclude that SIMU predicts the Ly_γ quasimolecular feature to be more prominent than BALROG. This might be explained by the fact that the extent of the $n = 4$ wave function is larger than that of $n = 3$, meaning that the probability that there is at least one ion inside the $n = 4$ is increased and there is a high probability that there is a second nearby particle strongly perturbing the atom. This probability has increased so much that the feature is as prominent as (if not more so) the traditional Ly_γ line shape.

C. H-like argon in fusion plasmas

Argon is commonly used in the diagnostics of fusion plasmas. We therefore apply these models to Ar^{17+} line shapes to

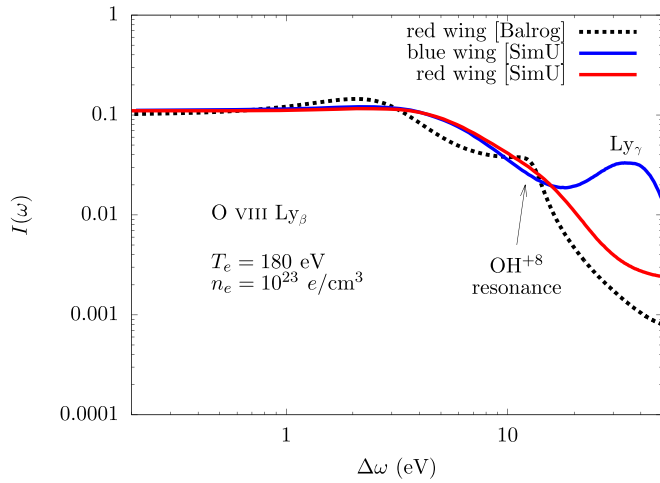


FIG. 6. Demonstration of the resonance in SIMU by plotting O VIII Ly_β in log-log scale. Compared to the BALROG calculation, the resonance in SIMU is substantially broader and redshifted due to ion dynamics and N -body effects, respectively.

see what impact penetrative collisions have; this is demonstrated in Fig. 7. We note that these fusion plasmas have substantially higher temperatures than what was explored in the base of the convection zone conditions. At much higher temperatures, the line shape is much more sensitive to the ion dynamics of the protons in the plasma. In fact, the reduction in the linewidth due to the penetrating collisions is only approximately 10%, an amount comparable to the reduction in the dipole-only calculation (approximately 15%). This would certainly indicate that the FWHM of Ar lines is insensitive to the composition of the plasma. The most significant changes

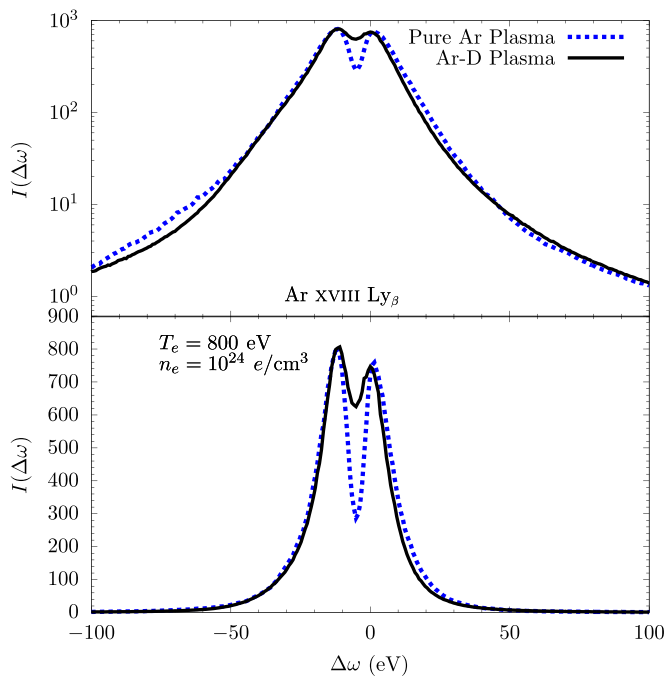


FIG. 7. Argon Ly_β calculation (SIMU) in a pure argon plasma vs a deuterium plasma. The resulting change in the line shape is comparable to that of Fig. 1.

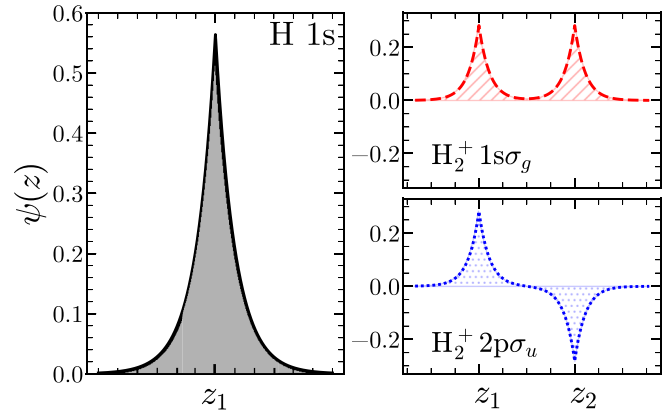


FIG. 8. Demonstration of parity splitting in molecular hydrogen. A slice of the electron wave function along the z axis is plotted for the ground state of H on the left and the first two steady-state solutions of H_2^+ on the right, with protons located at z_1 and z_2 .

are ones that are already seen (and expected) in the dipole approximation: The lighter element has a more significant ion dynamics effect that makes the dip shallower.

IV. DISCUSSION

The first problem these models face is that they are trying to model a multicenter problem with a single-center basis set. This is a challenge when working with a finite basis set. In this instance, the Schrödinger equation solver has difficulty reproducing the required molecular wave-function properties. Moving from a single-atom radiator to a multiatom radiator increases the number of allowed states. For a diatomic molecule, there is parity splitting (that is not present in a monatomic system) because the states can have either odd or even symmetry, and the electron can exist around either atom. This parity splitting is illustrated in Fig. 8 for steady-state solutions of H_2^+ . A finite single-center basis set cannot adequately represent these multicenter states. The consequence of this is that the predicted resonances are at the wrong energies. Figure 9 demonstrates how one of the strongest resonances in the H spectrum is off by nearly an entire eV. This statement does not rely on a theoretical justification but rather on an observational one. In white dwarfs, there is an H_2^+ resonance clearly identifiable at 1400 \AA .

Much effort can therefore be put into calculating the molecular structure. Allard and Koester [45] and Allard *et al.* [21] do just this. They make the Anderson-Talman approximation [46], where only binary collisions are considered and interperturber correlations are neglected. They also make the adiabatic approximation where the nearest proton is always aligned with the z axis, which would neglect the rotations of the plasma particles, an important broadening mechanism for Ly_α [47,48]. This method will reproduce the 1400-\AA feature seen in white-dwarf spectra, but the rest of the line is limited by not accounting for the N -body problem. Furthermore, these efforts have not simultaneously included the effect of the electrons, but instead rely on an approximate convolution procedure.

This issue with parity splitting may not be so severe in highly ionized elements with a mixture. This is because the resulting quasimolecular structure will not be diatomic and the

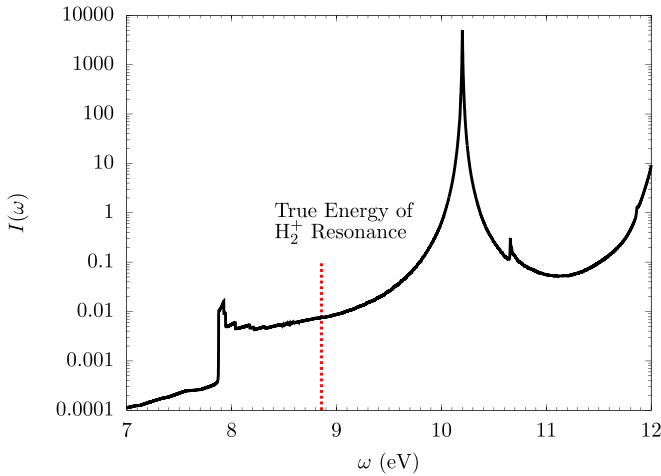


FIG. 9. BALROG calculation of the Ly_α and the associated H_2^+ resonances. This demonstrates that the current full Coulomb calculation poorly reproduces the molecular transition energy for H I Ly_α . SIMU (not shown) presents a resonance in the same location as BALROG, indicating that this is a problem with the method, not the calculation.

symmetry between the different particles is broken. We cannot state more about the level of accuracy for mixtures here.

It is also clear from this study that in extremely dense plasmas, the two-center treatment is insufficient to model the line shape adequately. To illustrate how significant the N -body effects are, we look at the Ar-H calculations. Figure 10 demonstrates where one expects the resonance to be and compares it against SIMU calculations. We chose to repeat the calculations of Fig. 7 but at a lower density where the nearest-neighbor approximation would be valid. However, ion dynamics has smoothed it out to be a barely perceptible feature. To confirm that what we see is indeed the quasimolecular feature, we increased the mass of the deuterium atoms to

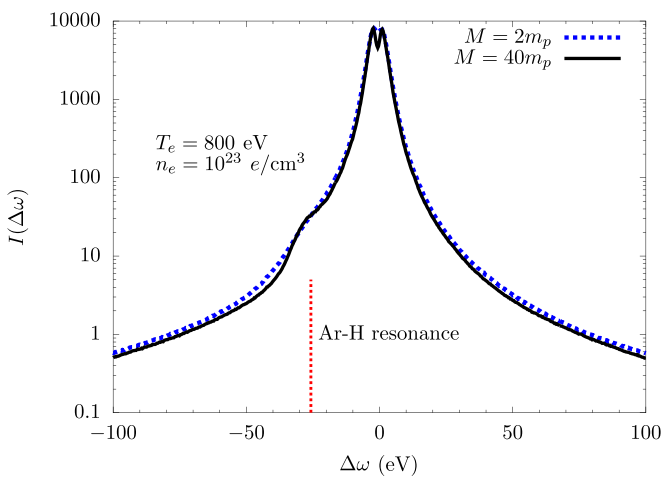


FIG. 10. Argon Ly_β line shape at a lower density. The nearest perturber approximation is more valid at this lower density, and a broad resonance can be seen. The broadness of the resonance is hard to pick out, so we increased the mass of the deuterium atoms to 40 times the mass of the proton to more clearly discern the quasimolecule resonance.

slow their motion through the plasma enough to distinguish the resonance clearly. It could be argued that there is some remnant of the resonance in the $n_e = 10^{24} \text{ e/cm}^3$ case in Fig. 7. However, if it is there, the feature is not prominent, being nearly 20 eV wide, and the peak has shifted from its zero-density frequency of $\Delta\omega = -25 \text{ eV}$ to about -40 eV . In this regime, the N -body effects dominate the resonance feature. We also point to the Ly_γ example in Fig. 5, where the quasimolecular resonance broadens the overall line rather than creating a resonance farther down the wing. The additional broadening of Ly_γ is not predicted by the binary-collision model of BALROG, indicating that this enhancement is only possible through multiple perturbing ions within R_{FC} .

With both of the methods presented, the deflection of the ion motion is ignored. When the ion penetrates the wave function of the radiating atom, the nucleus is no longer shielded entirely (in the case of neutrals). Therefore, the trajectory of the plasma ions is altered. This is less of a problem for highly charged radiators with a repulsive potential due to the long-range unscreened nuclear charge.

There is yet another important physical effect that has been omitted in these calculations: the effect of charge exchange. As is made clear from Fig. 8, when a plasma ion comes close, the electron can be shared between the two ion centers. This means that, in principle, we can model the probability that the plasma electron “steals” an electron from the initial radiator in a charge-exchange process. Neither SIMU nor BALROG includes charge exchange and both assume that the radiator electron always stays with the original nucleus.

Thus, as of now, there is no suitable model that captures all aspects of the problem. The existing models can either accurately account for the molecular structure or solve for the N -body effects, but they cannot account for both to the degree of accuracy desired.

V. CONCLUSION

The effect of penetrating ion collisions was explored here. Penetrating collisions do not significantly affect the widths of lines and may slightly affect the shifts. Any changes in the spectral linewidths due to composition are, for the most part, captured by dipole-only interactions. Where the penetration of ions into the radiator wave function has the most significant changes to the line shape are quasimolecular resonances in the far wings of the line. These resonances are sensitive to the composition of the plasma. The location of the resonances depends on the charge of the radiators in the plasma and the widths of the features depend on the ion dynamics.

These quasimolecular resonances are not going to be important from a diagnostic perspective. However, depending on the strength of the line, these features could impact opacity. It is well known that broader spectral lines will increase the Rosseland mean opacity of matter. These quasimolecular features put more opacity in the low-opacity region between the lines and, depending on the frequency-dependent opacity, may affect estimates of the Rosseland opacity. Currently, the tools employed by BALROG can be used to study multielectron systems. Still, SIMU, due to its analytic treatment of the full Coulomb problem, is limited to hydrogenic systems. More

work is certainly required to explore the full implications of the impact this work has on the far-wing opacity.

ACKNOWLEDGMENTS

T.A.G. and J.W. acknowledge support from the Wootton Center for Astrophysical Plasma Properties. This material is

based upon work supported by the National Nuclear Security Administration, Stewardship Science Academic Alliance, under Award No. DE-NA-003843. J.W. also acknowledges support from the U.S. Department of Energy National Nuclear Security Administration SSGF program under Grant No. DE-NA0003960.

-
- [1] P. B. Cho, T. A. Gomez, M. H. Montgomery, B. H. Dunlap, M. Fitz Axen, B. Hobbs, I. Hubeny, and D. E. Winget, *Astrophys. J.* **927**, 70 (2022).
- [2] I. Hubeny and T. Lanz, *Astrophys. J.* **439**, 875 (1995).
- [3] R. E. Falcon, G. A. Rochau, J. E. Bailey, T. A. Gomez, M. H. Montgomery, D. E. Winget, and T. Nagayama, *Astrophys. J.* **806**, 214 (2015).
- [4] C. Stollberg, E. Stambulchik, B. Duan, M. A. Gigosos, D. G. Herrero, C. A. Iglesias, and C. Mossé, *Atoms* **6**, 23 (2018).
- [5] T. A. Gomez, T. Nagayama, P. B. Cho, M. C. Zammit, C. J. Fontes, D. P. Kilcrease, I. Bray, I. Hubeny, B. H. Dunlap, M. H. Montgomery, and D. E. Winget, *Phys. Rev. Lett.* **127**, 235001 (2021).
- [6] R. E. Falcon, D. E. Winget, M. H. Montgomery, and K. A. Williams, *Astrophys. J.* **712**, 585 (2010).
- [7] P. Bergeron, P. Dufour, G. Fontaine, S. Coutu, S. Blouin, C. Genest-Beaulieu, A. Bédard, and B. Rolland, *Astrophys. J.* **876**, 67 (2019).
- [8] T. A. Gomez, T. Nagayama, P. B. Cho, D. P. Kilcrease, C. J. Fontes, and M. C. Zammit, *J. Phys. B: At. Mol. Opt. Phys.* **55**, 034002 (2022).
- [9] M. A. Gigosos, *J. Phys. D* **47**, 343001 (2014).
- [10] C. F. Hooper, *Phys. Rev.* **165**, 215 (1968).
- [11] C. A. Iglesias, H. E. DeWitt, J. L. Lebowitz, D. MacGowan, and W. B. Hubbard, *Phys. Rev. A* **31**, 1698 (1985).
- [12] W. L. Wiese, D. E. Kelleher, and V. Helbig, *Phys. Rev. A* **11**, 1854 (1975).
- [13] J. M. Luque, M. D. Calzada, and M. Sáez, *J. Phys. B: At. Mol. Opt. Phys.* **36**, 1573 (2003).
- [14] R. Stamm, E. W. Smith, and B. Talin, *Phys. Rev. A* **30**, 2039 (1984).
- [15] M. A. Gigosos and V. Cardenoso, *J. Phys. B: At. Mol. Phys.* **20**, 6005 (1987).
- [16] E. Stambulchik and Y. Maron, *J. Quant. Spectrosc. Radiat. Transfer* **99**, 730 (2006).
- [17] E. P. Nelán and G. Wegner, *Astrophys. J.* **289**, L31 (1985).
- [18] D. Koester, V. Weidemann, T. E. M. Zeidler, and G. Vauclair, *Astron. Astrophys.* **142**, L5 (1985).
- [19] B. Baschek, J. Koeppen, M. Scholz, R. Wehrse, A. Heck, C. Jaschek, and M. Jaschek, *Astron. Astrophys.* **131**, 378 (1984).
- [20] J. F. Kielkopf and N. F. Allard, *Astrophys. J. Lett.* **450**, L75 (1995).
- [21] N. F. Allard, A. Royer, J. F. Kielkopf, and N. Feautrier, *Phys. Rev. A* **60**, 1021 (1999).
- [22] L. A. Woltz and C. F. Hooper Jr., *Phys. Rev. A* **30**, 468 (1984).
- [23] S. Alexiou and R. W. Lee, *J. Quant. Spectrosc. Radiat. Transfer* **99**, 10 (2006).
- [24] G. C. Junkel, M. A. Gunderson, C. F. Hooper Jr., and D. A. Haynes Jr., *Phys. Rev. E* **62**, 5584 (2000).
- [25] B. F. Kraus, L. Gao, K. W. Hill, M. Bitter, P. C. Efthimion, T. A. Gomez, A. Moreau, R. Hollinger, S. Wang, H. Song, J. J. Rocca, and R. C. Mancini, *Phys. Rev. Lett.* **127**, 205001 (2021).
- [26] F. Sobczuk, K. Dzierżęga, and E. Stambulchik, *Phys. Rev. E* **106**, L023202 (2022).
- [27] J. E. Bailey, T. Nagayama, G. P. Loisel, G. A. Rochau, C. Blancard, J. Colgan, P. Cosse, G. Faussurier, C. J. Fontes, F. Gilleron, I. Golovkin, S. B. Hansen, C. A. Iglesias, D. P. Kilcrease, J. J. Macfarlane, R. C. Mancini, S. N. Nahar, C. Orban, J. C. Pain, A. K. Pradhan *et al.*, *Nature (London)* **517**, 56 (2015).
- [28] H. R. Griem, *Spectral Line Broadening by Plasmas* (Academic, New York, 1974).
- [29] E. W. Smith, J. Cooper, and C. R. Vidal, *Phys. Rev.* **185**, 140 (1969).
- [30] Spectral line shapes in plasmas workshops, <http://plasma-gate.weizmann.ac.il/sbsp/>.
- [31] D. B. Boercker, C. A. Iglesias, and J. W. Dufty, *Phys. Rev. A* **36**, 2254 (1987).
- [32] A. Calisti, C. Mosse, M. Koubiti, R. Stamm, and B. Talin, *J. Quant. Spectrosc. Radiat. Transfer* **54**, 89 (1995).
- [33] E. Stambulchik, D. V. Fisher, Y. Maron, H. R. Griem, and S. Alexiou, *High Energy Density Phys.* **3**, 272 (2007).
- [34] M. C. Zammit, D. V. Fursa, and I. Bray, *Phys. Rev. A* **82**, 052705 (2010).
- [35] E. Stambulchik and C. A. Iglesias, *Phys. Rev. E* **105**, 055210 (2022).
- [36] H. A. Bethe and E. E. Salpeter, *Quantum Mechanics of One- and Two-Electron Atoms* (Springer, Berlin, 1957).
- [37] T. A. Gomez, T. Nagayama, D. P. Kilcrease, M. H. Montgomery, and D. E. Winget, *Phys. Rev. A* **94**, 022501 (2016).
- [38] C. A. Iglesias, *High Energy Density Phys.* **38**, 100921 (2021).
- [39] L. A. Woltz and C. F. Hooper Jr., *Phys. Rev. A* **38**, 4766 (1988).
- [40] U. Fano, *Phys. Rev.* **131**, 259 (1963).
- [41] T. A. Gomez, T. Nagayama, C. J. Fontes, D. P. Kilcrease, S. B. Hansen, M. C. Zammit, D. V. Fursa, A. S. Kadyrov, and I. Bray, *Phys. Rev. Lett.* **124**, 055003 (2020).
- [42] E. Leboucher-Dalimier, P. Sauvan, P. Angelo, H. Derfoul, T. Ceccotti, P. Gauthier, A. Poquérousse, A. Calisti, and B. Talin, in *Spectral Line Shapes*, edited by R. M. Herman, AIP Conf. Proc. No. 467 (AIP, Melville, 1999), pp. 64–76.
- [43] T. Nagayama, J. E. Bailey, G. P. Loisel, G. S. Dunham, G. A. Rochau, C. Blancard, J. Colgan, P. Cossé, G. Faussurier, C. J. Fontes, F. Gilleron, S. B. Hansen, C. A. Iglesias, I. E. Golovkin,

- D. P. Kilcrease, J. J. MacFarlane, R. C. Mancini, R. M. More, C. Orban, J. C. Pain *et al.*, [Phys. Rev. Lett. **122**, 235001 \(2019\)](#).
- [44] J. E. Bailey, G. A. Rochau, R. C. Mancini, C. A. Iglesias, J. J. Macfarlane, I. E. Golovkin, C. Blancard, P. Cosse, and G. Faussurier, [Phys. Plasmas **16**, 058101 \(2009\)](#).
- [45] N. F. Allard and D. Koester, *Astron. Astrophys.* **258**, 464 (1992).
- [46] A. Royer, [Phys. Rev. A **22**, 1625 \(1980\)](#).
- [47] A. Calisti, A. Demura, M. Gigosos, D. González-Herrero, C. Iglesias, V. Lisitsa, and E. Stambulchik, [Atoms **2**, 259 \(2014\)](#).
- [48] E. Stambulchik and A. V. Demura, [J. Phys. B: At. Mol. Opt. Phys. **49**, 035701 \(2016\)](#).